River Systems Vol. 20/3–4, p. 169–183
published online September 2012

Article

Evaluating the effect of temperature induced water viscosity and density fluctuations on virus and DOC removal during river bank filtration – a scenario analysis

Julia Derx[1,2,5]*, Andreas H. Farnleitner[2,3,5], Matthias Zessner[2,4], Liping Pang[6], Jack Schijven[7,8] & Alfred P. Blaschke[1,2,5]

with 9 figures and 10 tables

Abstract: Riverbank filtration is considered an efficient method for removing contaminants from infiltrated surface water in the subsurface. Despite indications that changing water temperatures affect the biochemical and biological mediated removal processes of contaminants, the impact of temperature induced fluid viscosity and density effects on contaminant removal during riverbank filtration is not well understood. This paper investigates the viscosity and density effects associated with seasonal changes in groundwater temperature on virus and dissolved organic carbon (DOC) removal during riverbank filtration. Hypothetical aquifer and flood wave scenarios were assumed. Data on groundwater temperature were taken from an Austrian field site of the River Danube recorded during 2010/2011. Based on removal rates taken from previously published field experiments, virus and DOC transport was simulated for highly permeable gravel, fine gravel and fine sandy gravel material. Our simulations indicate that for DOC and a wide range of virus types the viscosity and density effects induced by water temperature changes can counteract with temperature dependent decay and inactivation rates. For particular situations, however, such as for receding floods during colder periods, our simulations indicate that fluid viscosity and density effects can result in a net decrease in the virus removal efficiency during colder periods. Persistent types of viruses (e.g. *polio 1* or *HAV*) can be reduced less effectively and may travel by up to 25 % faster during warmer than during colder periods. Our simulations indicate that viscosity and density effects induced by temperature changes should be considered for studying and simulating virus or DOC removal and transport during riverbank filtration. The effects may be important specifically at field sites with a high river-aquifer exchange and large variations in groundwater temperature.

Keywords*:* Riverbank filtration, DOC transport, virus transport, water temperature

Authors' addresses:
[1]Institute of Hydraulic Engineering and Water Resources Management, Vienna University of Technology
[2]Centre for Water Resource Systems, Vienna University of Technology
[3]Institute for Chemical Engineering, Research Area Applied Biochemistry and Gene Technology, Research Group Environmental Microbiology and Molecular Ecology, Vienna University of Technology, Vienna, Austria
[4]Institute of Water Quality, Resources and Waste Management, Vienna University of Technology, Vienna, Austria
[5]Interuniversity Cooperation Centre Water and Health (ICC); www.waterandhealth.at
[6]Institute of Environmental Science & Research Ltd, P.O. Box 29181, Christchurch, New Zealand
[7]Expert Centre for Methodology and Information Services, National Institute of Public Health and the Environment (RIVM), P.O. Box 1, 3720 BA Bilthoven, The Netherlands
[8]Department of Earth Sciences, Utrecht University, P.O. Box 80021, 3508 TA Utrecht, The Netherlands
*Corresponding author: derx@hydro.tuwien.ac.at

www.schweizerbart.de
DOI: 10.1127/1868-5749/2012/0059
1868-5749/2012/0059 $ 7.20

1. Introduction

In the view of the increase in world population, the demand for efficient treatment methods for drinking water has increased. The potential capacity of riverbank filtration to effectively remove contaminants has been demonstrated. However, during floods river water was found to infiltrate more quickly and at a higher rate into the riverbank, posing an increased risk for groundwater contamination (e.g. Shankar et al. 2009). A study of river-groundwater interaction at the River Danube indicated that flood events can lead to enhanced river-aquifer mixing and thus to facilitated transport of solutes into groundwater (Derx et al. 2010). The authors suggested that transient, three-dimensional variations in pore velocities may be responsible.

Other factors which can influence river-aquifer exchange flow rates were identified, such as bed form heterogeneities (Storey et al. 2003) or meandering of rivers (Peyrard et al. 2008, Cardenas 2008, Boano et al. 2010).

Water temperature was also found to significantly affect the infiltration capacity from rivers (Blaschke et al. 2003, Hubbs et al. 2007). Hubbs et al. (2007) found that wide variations in water viscosity associated with temperature resulted in the doubling of the infiltration capacity from winter to summer at the Ohio River. They recommended that the rated capacity of riverbank filtration systems should be considered as a range between coldest and warmest water conditions. Similarly, Blaschke et al. (2003) found that seepage rates from the River Danube vary substantially throughout the year and estimated that 50 % are due to variations in water viscosities between summer and winter. It is yet unclear, how changing viscosities and densities throughout the year would affect contaminant removal during soil passage. Several studies exist which investigated the effects of water temperature on the reduction of nitrate, sulphate, organic compounds and pathogenic viruses during soil passage. The parameters that were considered to change with water temperature included the redox potential (Gross-Wittke et al. 2010, Schwarzenbach et al. 1983), the virus inactivation and attachment rates (Schijven & Hassanizadeh 2000, Yao et al. 1971) or the DOC decay rates (Jekel et al. 2009). The effects of changing viscosities and densities on contaminant transport, however, were previously disregarded. As contaminants, waterborne pathogenic viruses are one contaminant of major concern because of a high persistence in the aqueous environment, an ease of transportation in groundwater and low infectious doses (Schijven & Hassanizadeh 2000, Stalder et al. 2011). Dissolved organic carbon (DOC) is further an often used surrogate for organic pollutants.

During changing hydraulic flow conditions, such as during floods or during pumping, groundwater temperature may respond strongly to river water temperature because of higher water level gradients and thus more heat convection (Su et al. 2004). During floods viruses and DOC may travel further into groundwater because of a reduced groundwater travel time and an increased fraction of freshly infiltrated river water. During such conditions, fluid viscosity and density variations may therefore affect virus and DOC concentrations in groundwater even stronger.

From these perspectives it is therefore important to understand the effects of floods combined with variations in water viscosities and densities on contaminant removal.

The primary objective of this paper was to investigate how viscosity and density effects combined with changing hydraulic conditions can affect virus and DOC removal during riverbank filtration and soil passage. Hypothetical aquifer and flood wave scenarios were assumed with simplified aquifer and river geometries in order to exclude other interfering effects which may occur at real field sites. These scenarios are considered as a first step for investigating if viscosity and density changes have an important effect on contaminant removal during soil passage and should thus be considered in the future.

A secondary objective of this paper was to investigate the effects of temperature dependent virus inactivation and DOC decay rates on virus and DOC transport and how they relate to viscosity and density effects induced by changes in water temperature. Even though virus inactivation rates usually increase with water temperature, they can vary strongly for different types of viruses. For example, persistent types of viruses exist also with very low inactivation rates independently from water temperature (Schijven et al. 2002). The relation of DOC decay to water temperature, however, is well known from waste water treatment practice. Both virus inactivation and DOC decay rates were therefore assumed dependent on water temperature independently and in combination with fluid densities and viscosities. A third objective was to discuss the general implications of our results for the consideration of contaminant removal during riverbank filtration.

2. Description of the water flow and transport model

The groundwater flow and transport were simulated in three dimensions (SUTRA2.1, Voss & Provost 2008), coupled to 1D surface water simulations (HEC-RAS, U.S. Army Corps of Engineers 2008), fully accounting for transient, variably saturated flow conditions. The simulations in three dimensions were required because the near-river groundwater flow directions respond to a flood wave in directions parallel and perpendicular to the river axis

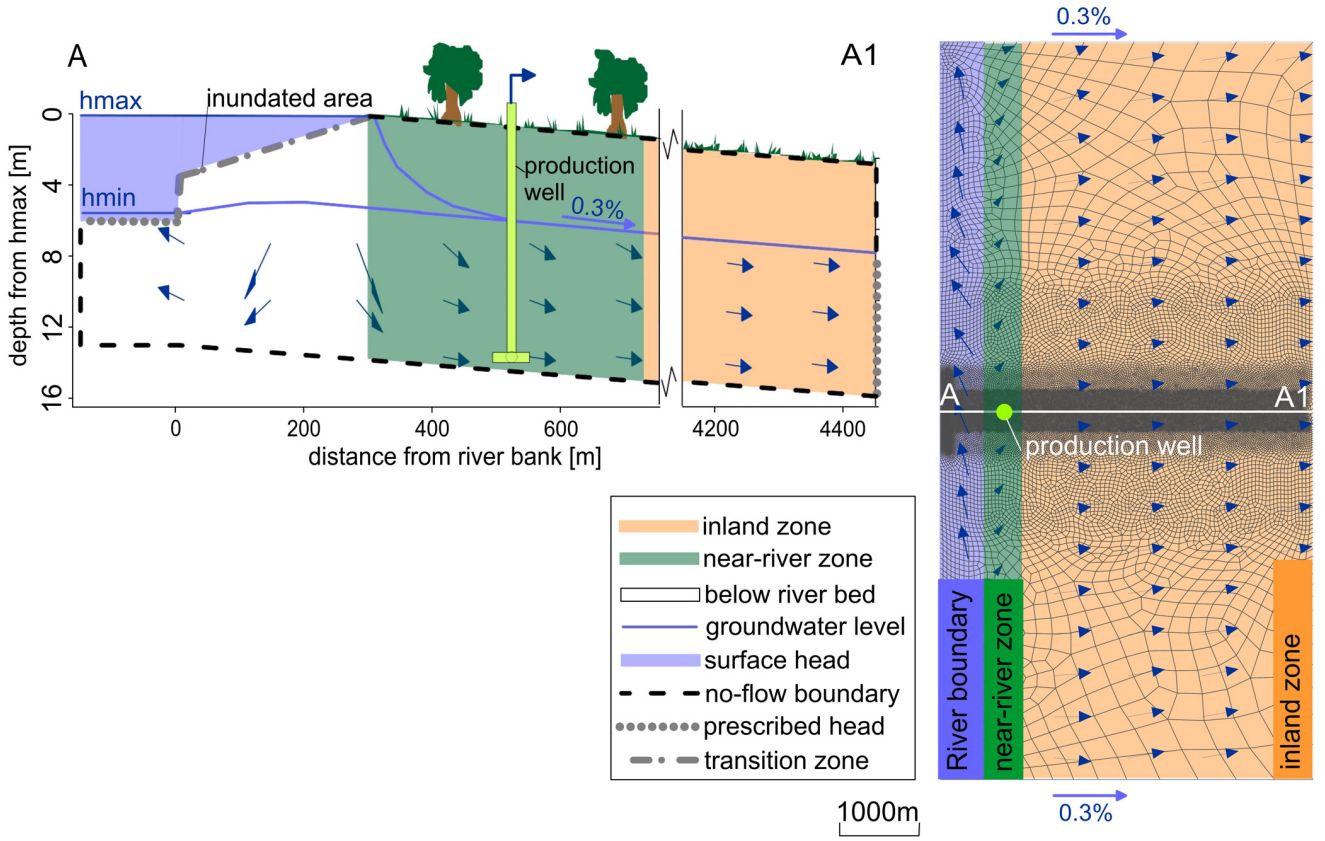

Fig. 1. Hypothetical aquifer scenarios assumed in the simulations. Map view (left) and cross section A-A1 (right) of the model setup. 3 spatial zones are indicated, the inland (red), near-river zone (green) and the zone below the river bed (white). In each of these zones the same, time-dependent fluid viscosities and densities were assigned for the scenario simulations.
Min and max river water levels during scenario simulations together with simulated groundwater levels are indicated; The location of the drinking water well and the boundary conditions are shown: $h(t) = h_{river,\,t}$; no-flow boundary: $q = 0$; and transition zone, where either $h(t) = h_{river,\,t}$ if $h_{river,\,t} > h_{groundsurface}$ or $q = 0$ if $h_{river,t} \leq h_{groundsurface}$ (Derx et al. 2010).

and in vertical direction, as can be seen from the simulated groundwater flow directions after 20 d of simulation time in Figure 1. The general form of the 3-D variably saturated groundwater flow equation as solved in SUTRA2.1 is

$$(\Theta_w \rho s_{op} + \Theta \rho_T \frac{\partial \Theta_w}{\partial p}) \cdot \frac{\partial p}{\partial t} - \vec{\nabla}[\frac{\rho_T K(\Theta_w)}{\mu_T}(\vec{\nabla} p + \rho_T \vec{g})] + q_w = 0 \quad (1)$$

Notations are given in Table 1. The water density ρ_T and the dynamic viscosity μ_T were assumed dependent on water temperature T. The model geometry and the boundary conditions are shown in Figure 1. For the assumed distribution of groundwater temperature in our scenarios, see Section 4. Based on a specific groundwater temperature at a respective time and location, ρ_T and μ_T were calculated by linear interpolation between a range of values from 2–22 °C (Table 2). The water flow model was tested for a field site at the Austrian Danube with transient flow conditions during several flooding events. It was demonstrated that the transient groundwater flow situation during flooding events could be reproduced, with mean biases always less than 7 cm (Derx et al. 2010). For a detailed description of the water flow model coupled with transient surface water – groundwater interaction, see Derx et al. (2010).

The transport simulations were based on the advection-dispersion equation with a first-order reduction rate (λ) and virus inactivation rate (η) solved by SUTRA2.1 (Voss & Provost 2008):

$$\frac{\partial \Theta \Theta_w \rho_T C}{\partial t} + \vec{\nabla}(\Theta \Theta_w \rho_T \vec{v} C) - \vec{\nabla}(\Theta \Theta_w \rho_T D \vec{\nabla} C) = -\Theta \Theta_w \rho_T \lambda C - \Theta \Theta_w \rho_T \eta C \quad (2)$$

Notations are given in Table 1. As for the water flow model, the water density ρ_T was assigned dependent on water temperature. SUTRA2.1 was tested and verified for

Table 1. Notation.

C	concentration of free viruses (pfu/l) or DOC (mg/l)
DOC	dissolved organic carbon
D	3-D dispersion tensor (m^2/s)
g	gravity vector (ms^{-2})
$\vec{K}$	3-D aquifer permeability matrix (m^2)
K_f	hydraulic conductivity (m/s)
$K^*_{f,v/h}$	anisotropy ratio of hydraulic conductivity (–)
λ	DOC decay rate of the adsorbable and biodegradable portion and virus removal rate (d^{-1})
λ_s	virus log removal rate (log_{10}/m)
p	hydraulic water pressure (kN/m^2)
pfu/l	virus particle forming units per litre
q_w	fluid mass sink (mass fluid per time and volume aquifer, kg/m^3s)
s_{op}	specific pressure storativity $(kg/ms^2)^{-1}$
t	simulation time (d)
T	water temperature (°C)
v	pore velocity (m/s)
$\vec{\alpha}_l$	longitudinal dispersivity (m)
α_t	transversal dispersivity (m)
$\alpha^*_{v/h}$	anisotropy ratio of dispersivity (–)
η	virus inactivation rate (d^{-1})
$\vec{\nabla}$	differential operator (–)
ρ_T	fluid density (999.7 kg/m^3 at 10 °C)
Φ	effective porosity (–)
Φ_r	residual water saturation (–)
Φ_w	water saturation (volume of water per volume of voids, –)
μ_T	fluid viscosity (1.307×10^{-3} kg/ms at 10 °C)

several 2-D/3-D variable-density solute transport problems by Voss & Provost (2008). In order to test the simulations with first-order concentration reduction, a simple box model was set up. Initial solute concentrations at one uniform value were assigned throughout the box and a first-order decay rate was specified. The concentration reduced exponentially with time (results not shown).

3. River and aquifer system, model parameters and data used for the scenarios

Hypothetical river and aquifer scenarios were assumed in a temperate, continental climatic region with a variation in river water temperature from 2 °C to 25 °C throughout the year. A large river was assumed with an oxygen content close to saturation which is important for assuming decay rates in our DOC transport simulations (Section 3.1). A flood wave scenario was assumed with an increase in water level by 5 m. The corresponding river flow discharges range between 100 and 5700 m^3/s. For comparison, such flooding events may occur at large rivers on average once a year (for example at the River Danube, see via donau, 1997). The unconfined alluvial aquifers were assumed fully connected to the river and 10 m deep, consisting of gravel, fine gravel and fine gravel porous media with sand. These conditions are frequently found at riverbank filtration sites underlaid by fluvial gravel aquifers (Hoehn 2002, Homonnay 2002, Weiss et al. 2005).

As the hydraulic conductivity in fluvial gravel aquifers near rivers often ranges from 10^{-3} m/s to 10^{-2} m/s (e.g. the River Rhine, Schubert 2006 and Shankar et al. 2009), this range was assumed in the simulations. An effective porosity of 0.1 was assigned for the scenarios, which is on the conservative side of the range reported for gravel by de Marsily (1986) (0.1–0.2). The dispersivity values for the horizontal directions (α_l) were taken from the results of tracer tests conducted in the Seewinkel nearby Lake Neusiedl where the soil properties are similar to the assumed scenarios (Kroiss et al. 2002). α_l was set to 5 m in all simulations. Anisotropy ratios of hydraulic conductivity ($K^*_{f,v/h}$) and dispersivity ($\alpha^*_{v/h}$) of 0.1 were assumed for the scenarios (Chen 2000, Gelhar et al. 1992).

The groundwater temperature assumed in our scenarios was based on continuous water temperature data near the Austrian River Danube (Fig. 2). We chose this specific site because of characteristics similar to our assumed river and aquifer system. During the monitoring period from December 2009 to September 2011 two flood events occurred with an increase in river water level by 5 m, one in summer and one in winter. Even though no floods were recorded in spring nor autumn,

Table 2. Dynamic viscosity and water density as functions of water temperature (Kozeny 1953, Geiseler 1967). $\mu_{10°C} = 1.307\times10^{-3}$ kg/ms.

T (°C)	2	8	10	12	14	16	22
$\mu_{10°C} / \mu_T$	0.79	0.94	1.00	1.06	1.11	1.17	1.36
ρ_T	999.94	999.85	999.70	999.50	999.24	998.94	997.77

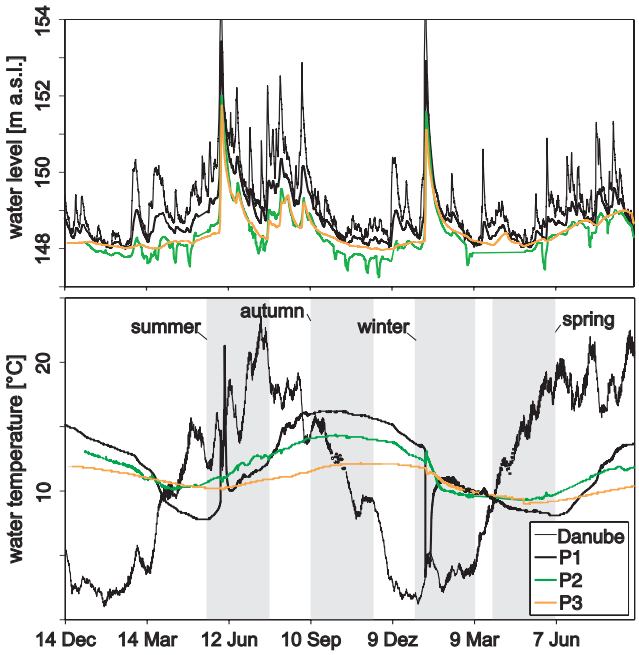

Fig. 2. Observed water level (top) and water temperatures in the Austrian Danube River and in groundwater 140m (P1), 390m (P2) and 1400m (P3) from the river from Dec 2009 to Sep 2011; For scenario simulations, transient fluid viscosities and densities were assigned based on water temperature data (May 29–Jul 28, 2010 for a flood in summer, Sep 10–Nov 11, 2010 for a flood in autumn, Jan 10–Mar 11, 2011 for a flood in winter and Apr 11–Jun 06, 2011 for a flood in spring, as indicated in gray shading); Recorded time interval is 1 hour.

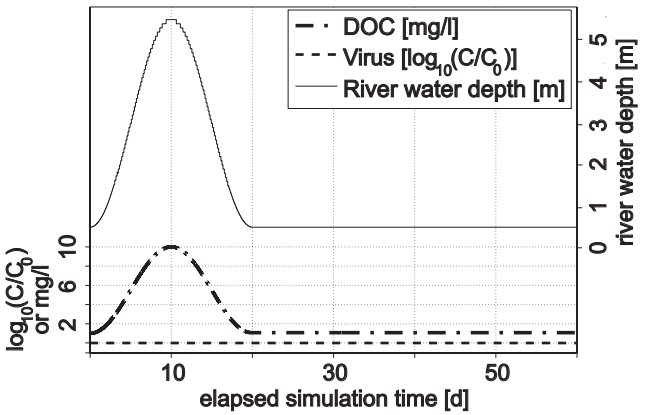

Fig 3. Water depth, virus and DOC concentrations at the river boundary assumed for scenarios. Virus concentrations are given in $\log_{10}\frac{C}{C_0}$, referring to the virus concentration C relative to an arbitrary initial concentration C_0 in the river.

the water temperature in the near-river aquifer approached twice the river water temperature during these seasons, similarly as during the floods. We therefore could assume the same distribution of groundwater temperatures during an increase in river water level by 5 m at the beginning of these time periods.

3.1. The fate of viruses and DOC in groundwater

The virus removal and DOC biodegradation rates used for our scenarios were based on previously published field experiments and on monitoring data in aquifers with similar characteristics as our assumed river and aquifer system (Section 3). Viruses of concern were any type of human waterborne pathogenic virus that could enter the groundwater system. Common types of human viruses found in groundwater which may affect the human body are: *adeno*, *echo*, *coxsackie*, *entero*, *hepatitis*, *polio*, *calici* and *rotaviruses* (Sim & Chrysikopoulos 1998).

The virus removal rates were based on published data from MS2 and PRD-1 bacteriophage field tracer experiments in fine gravel and coarse sand (Pang 2009, see Table 3). We selected MS2 and PRD1 as model viruses, as they are about equally conservative for attachment (Schijven and Hassanizadeh 2000). The virus removal rates were assumed constant and comprised attachment and some effect of inactivation and dilution. Virus inactivation rates (η) were assumed to change with water temperature. A relationship of $\ln(\eta) = 0.12\ T - 3.5$ was taken from Schijven & Hassanizadeh (2000) (p. 101) for *MS2* bacteriophages at water temperatures from 5 to 23 °C. The aquifer was assumed to be initially free of viruses and at the river boundary a constant virus concentration reduction of 0 $\log_{10}\frac{C}{C_0}$ was assumed (Fig. 3).

DOC is removed in groundwater due to adsorption and biodegradation processes (Partinoudi & Collins 2007). We assumed DOC decay rate constants (λ) for our scenarios based on published field experiments in gravel and sandy gravel aquifers (Table 4). From waste water treatment practice DOC decay rates are known to increase with water temperature due to an increase in microbial activity. The assumed DOC decay rate λ was based on a water temperature of 15 °C and was linearly interpolated from 0.61λ at 5 °C to 2λ at 25 °C, based on results from large column experiments (Jekel et al. 2009). DOC concentrations in rivers were found to vary strongly in space and time and to increase during flood events (e.g. in the Austrian Danube, Wolfram & Humpesch 2003, Wolfram & Humpesch 2004 and Wolfram & Humpesch 2005). Based on these studies, DOC concentrations in the river were assumed to increase from 1–10 mg/l during a flood event in our scenarios (Fig. 3). The initial concentrations

Table 3. Calculation of virus removal rates (λ) from field data encompassing the full range observed in sandy gravel and gravel media with MS2 and PRD1 bacteriophage tracers (Pang 2009); Bold λ values relate to values after correction for dilution and indicate the maximum or minimum values considered in the simulations (Section 4).

Reference	Source	Aquifer	Phage	λ (log_{10}/m)	v_{min} (m/d)	λ (d^{-1})	$r^2_{lin.}$ (–)	no. (–)	dilution corr.
Bales et al. 1995	Sewage	Sand, fine gravel	PRD-1	0.18	0.2	**0.07**	0.83	6	yes
Blanford et al. 2005	Sewage	Sand, fine gravel	PRD-1	0.89	0.5	1.09	lin.	31	no
Blanford et al. 2005	Sewage	Sand, fine gravel	PRD-1	0.11	0.5	0.13	lin.	21	no
Blanford et al. 2005	Tracer	Sand, fine gravel	PRD-1	0.12	0.5	0.14	lin.	32	no
DeBorde et al. 1998b	Septic tanks	Sand, gravel	MS2	0.39	1.0	0.90	0.84	3	no
DeBorde et al. 1999	Tracer	Sandy gravel	MS2	0.10	23.0	5.26	0.99	4	no
DeBorde et al. 1999	Tracer	Sandy gravel	PRD-1	0.09	26.0	5.66	0.98	4	no
Pieper et al. 1997	Tracer	Sand, fine gravel	PRD-1	0.22	0.8	0.40	0.77	4	no
Pieper et al. 1997	Sewage	Sand, fine gravel	PRD-1	0.21	0.4	0.20	0.43	4	no
Woessner et al. 2001	Tracer	Sand, gravel	PRD-1	0.01	115	3.19		1	no
Woessner et al. 2001	Tracer	Sand, gravel	MS2	0.04	147	**10.15**		1	yes

of DOC in groundwater were assumed low with 1 mg/l, as typically found in groundwater wells nearby rivers (e.g. near the River Thur, Hoehn & Scholtis 2011, the River Rhine, Schmidt et al. 2003 and the Ohio River, Weiss et al. 2003). DOC and viruses were assumed to be homogeneously distributed in the river in our scenarios (the river is shaded blue in Figure 1).

4. Scenario simulations

Scenarios for a flood in summer, in autumn, in winter and in spring were assumed with an increase in river water level by 5 m (Figure 3). We chose a simulation time long enough for investigating the contaminant breakthrough during and after the flooding event (60 d).

For the simulations, the hydraulic conductivity (K_f), virus removal and DOC decay rate (λ) were varied within ranges previously observed in gravel materials (Section 3 and Table 3 and 4). Respective minimum, median and maximum values of these parameters were assigned to highly permeable gravel, fine gravel and fine sandy gravel and all other parameters were left constant. The smallest λ values were assigned to highly permeable gravel material, the median values to fine gravel material and the largest values to fine gravel material with sand because of a higher affinity to attach to sediments (see Table 5).

As a simplified assumption, we divided the hypothetical aquifer into an inland zone, a zone near the river and a zone below the river bed (Fig. 1). For each of these zones we assigned the observed groundwater temperatures in piezometer P1 to the zone below the river bed, in piezometer P2 to the near-river zone and in piezometer P3 to the inland zone. Additionally, we assumed a well 500 m from the riverbank, consisting of concrete pipes which are 20 m long and extend radially 1 m above the bottom of the unconfined aquifer (horizontal wells, Fig. 1).

We assumed a pumping rate of 0 or 100 l/s. Virus inactivation and removal rates and DOC decay rates were assumed constant ($\eta = 0.02\ d^{-1}$; For values of λ, see Table 5). For additional scenarios for virus transport we assumed η to change with water temperature and also λ for DOC transport and the respective parameters com-

Table 4. Published decay rate constants from non-linear regression analyses to observed degradation curves of DOC and other organic compounds in aerobic sandy gravel aquifers.

Compound	Reference	Location	Aquifer type	λ (d^{-1})
DOC	Jekel et al. (2009)	30 m column	sandy and fine gravel	0.02–0.07
DOC	Kroiss et al. (2002)	Lake Neusiedl Austria	sandy gravel	0.02–0.04
benzene, paraxylene, naphthalene	Boggs et al. (1993)	MADE field site	gravelly sand	0.01–0.02
linear alkylbenzene -sulfonates	Krueger et al. (1998)	Cape Cod, MA	sand and gravel	0.01–0.07

Table 5. Input parameters and their values for assumed scenarios in coarse gravel, fine gravel and fine sandy gravel.

Soil type	gravel	fine gravel	fine sandy gravel
K_f (m/s)	10^{-2}	5×10^{-3}	10^{-3}
$\lambda_{15°C}$ (virus, d^{-1})	0.07	0.90	10.14
$\lambda_{15°C}$ (DOC, d^{-1})	0.01	0.02	0.07

Table 6. Hypothetical aquifer scenarios assumed and corresponding Figures showing the simulation results. Each scenario was simulated in coarse gravel, fine gravel and fine, sandy gravel, with an increase of river water level by 5 m.

Parameters dependent on water temperature	Pumping rate	Figures
viscosity, density	0 l/s	4,6(top),9(top)
viscosity, density	100 l/s	7
virus inactivation	0 l/s	6(middle)
viscosity, density, virus inactivation	0 l/s	6(bottom)
DOC decay	0 l/s	9(middle)
viscosity, density, DOC decay	0 l/s	9(bottom)

bined with fluid viscosity and density. For a complete list of assumed scenarios, see Table 6.

For each scenario, the virus $\log_{10}\frac{C}{C_0}$ concentration reductions were simulated, which were defined as the virus concentration C in groundwater relative to an arbitrary virus concentration in the river C_0. For DOC transport absolute concentrations were simulated in mg/l.

5. Results

5.1. Attenuation of water temperature fluctuation and exchange flow rates

The observed water temperature from December 2009 to September 2011 ranged from 2–25 °C in the River Danube (Fig. 2). The groundwater temperature fluctuations clearly attenuated and showed an increased time lag with increasing distance from the river. When comparing the observed peak water temperatures in the river and in groundwater, the time lags were from 72 to 117 d.

In order to quantify the effects of fluid viscosity and density variations on infiltration and exfiltration flow rates across the riverbed [m^3/s], they were calculated during the flooding event as the sum over the submerged zone shown in Figure 1. The transient simulation results showed that for both infiltration (+) and groundwater exfiltration (–) the exchange rates vary strongly with time. The exchange flow rates for coarse gravel, fine gravel and fine sandy gravel material during a summer flood varied from 0.3 to 7.3 m^3/s, –0.3 to 0.7 m^3/s and –0.5 to 1.9 m^3/s, respectively. They peaked on day 10 after rapidly rising river levels. The exchange flow rates varied from 3 to 34 % between the different seasons.

5.2. Simulated virus travel time and concentration reduction

For investigating the virus concentration reduction over time, we chose observation points from 320 to 1500 m from the river. The virus particles were transported from the river into groundwater. As soon as the virus particles had arrived at a respective point the simulated virus concentrations increased, thus their reduction decreased (Fig. 4). The simulated virus travel time was by up to 25 % (5 days) shorter in autumn than in spring (1500 m from the river bank, Fig. 4 top left). When the river water level decreased during the receding flood, the groundwater flow direction turned temporarily leading to groundwater exfiltration conditions in the river (see indicated groundwater flow directions after 20 d in Figs 1 and 5). Such conditions often occur, if the river water level decreases faster than the groundwater levels nearby the river. As a consequence, simulated virus concentrations were reduced after a simulation time of ≥ 15 days at a distance of 300–600 m from the river bank (Fig. 4 centre and right).

If the virus inactivation rates were assumed dependent on groundwater temperature, simulated virus concentrations were reduced by up to 2–5 $\log_{10}\frac{C}{C_0}$ more effectively (Fig. 4 middle left). The inactivation rate became less important for simulations the higher the assumed virus removal rates (0.9 and 10 d^{-1}, see Figure 4 middle centre and right). Simulation results for all effects combined show that fluid viscosity and density effects can cause a by 25 % earlier net arrival of virus particles (1500 m from the river bank, Figure 4 bottom left).

In our simulations fluid viscosity and density effects caused that the virus concentration reductions in coarse gravel differed by up to 1.3 $\log_{10}\frac{C}{C_0}$ between the seasons. The greatest effects were shown in coarse gravel material at 2500 m distance from the river bank and in fine gravel material at 700 m from the river bank (Fig. 6 top left and centre and Tables 7 and 8 top right). The effects were negligibly small in fine sandy gravel (Figs 6 right and Table 9). The scenario results further demonstrate that the required distances from the river to achieve a respective virus concentration reduction can differ accordingly over the seasons due to fluid viscosity and density effects. If virus inactivation rates and fluid viscosity and density

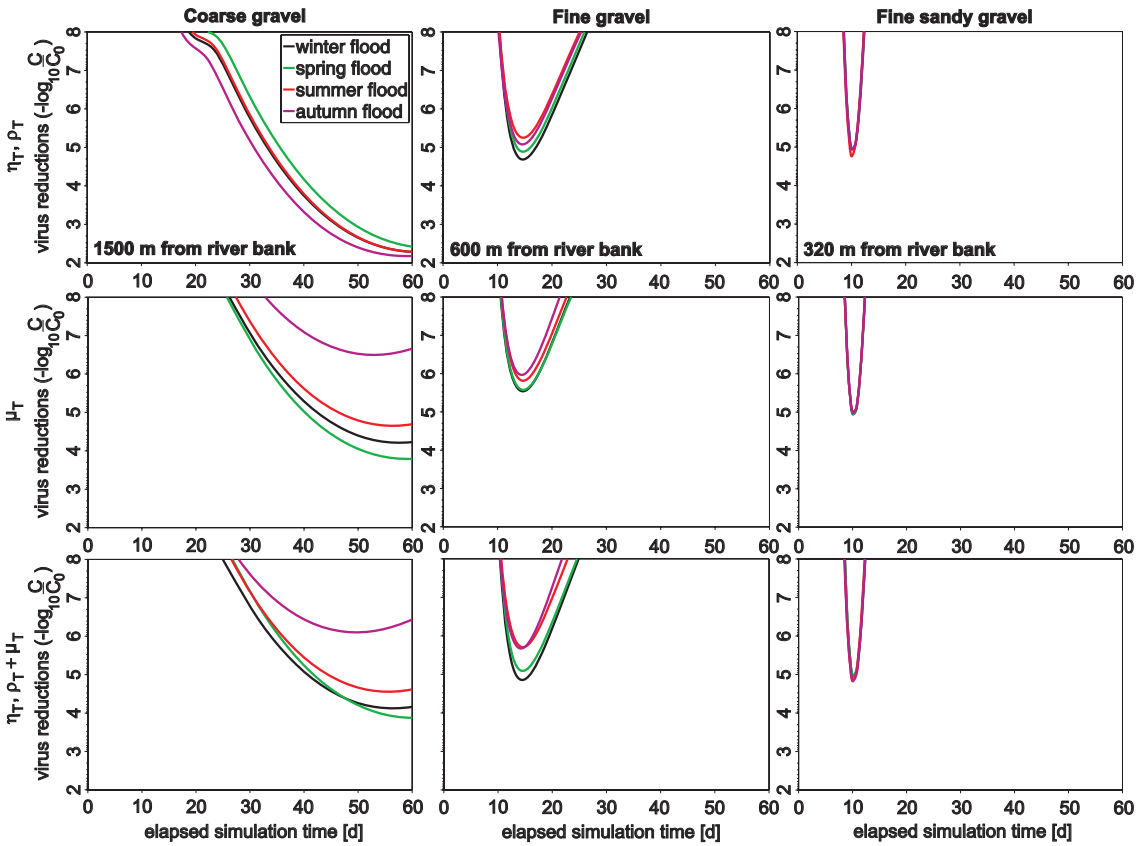

Fig. 4. Time plots of simulated virus concentrations at various distances from the river for coarse gravel, fine gravel and fine gravel with sand; For scenarios fluid viscosity (μ_T) and density (ρ_T, top), virus inactivation rate (η, middle) and all combined (bottom) were assigned dependent on water temperature. A pumping rate of 0 l/s is assumed; Each curve refers to the aquifer depth where the absolute minimum virus reduction was recorded;

were assumed dependent on water temperature, the simulated virus concentrations differed by up to 2.1 $\log_{10}\frac{C}{C_0}$ over the seasons. Fluid and viscosity effects were responsible of 38 % of this difference in simulated virus concentrations (compare Fig. 6 middle and bottom left). For the specific case in fine gravel fluid viscosity and density effects caused a net increase in virus concentrations by 5–10 % during colder periods (compare Fig. 6 middle and bottom centre).

The simulated virus concentrations were reduced by up to 0.5 $\log_{10}\frac{C}{C_0}$ less with pumping at a rate of 100 l/s than without pumping (Figs 6 and 7). An exception are the scenarios in coarse gravel, where viruses were transported far beyond the location of the well and pumping caused that fresh water was transported from inland. As a consequence the simulated virus concentrations were more reduced, by up to 0.5 $\log_{10}\frac{C}{C_0}$, than without pumping (Figs 6 and 7).

5.3. Simulated DOC travel time and concentration

The simulation results for DOC indicate that fluid viscosity and density effects can cause that DOC concentrations arrive by up to 14 % earlier in autumn than in spring (when comparing time of first arrival or time of concentration peaks, see Figure 8). Changing fluid viscosities and densities can further cause that the simulated DOC concentrations differ by up to 10 % over the seasons and the required distance from the river accordingly (Fig. 9 top and Tables 7 to 9 bottom).

When assuming that the DOC decay rate (λ) increases with water temperature, while fluid viscosity and density are kept constant, the simulation results show the opposite effect on DOC concentrations (Figs 8 and 9 middle). As a result the simulated DOC concentrations can differ less over the seasons (Fig. 9 middle and bottom). Fluid viscosity and density effects, however, caused that simulated DOC concentrations arrived by up to 14 % earlier (compare Fig. 8 middle and bottom).

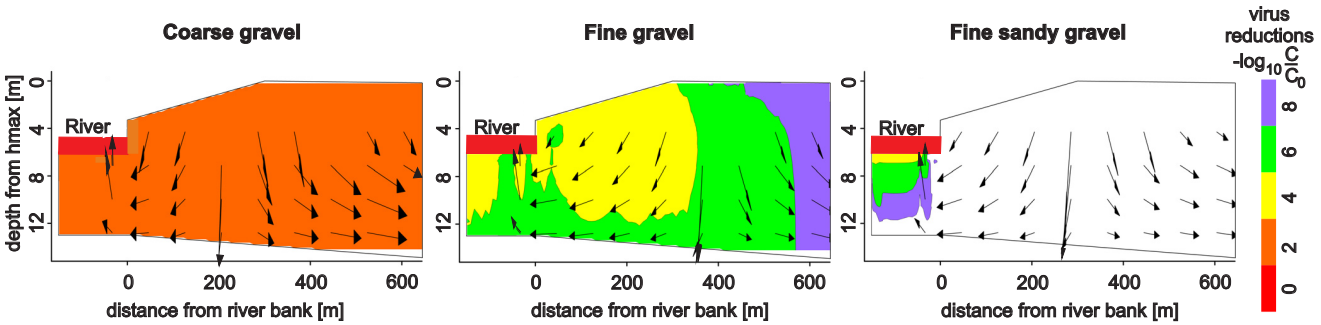

Fig. 5. Cross sections A-A1 (Fig. 1) of simulated virus concentrations (colors) and groundwater flow directions (black arrows) after 20 d of simulation time; Simulation results for coarse gravel (left), fine gravel (centre) and fine sandy gravel (right); A pumping rate of 0 l/s is assumed;

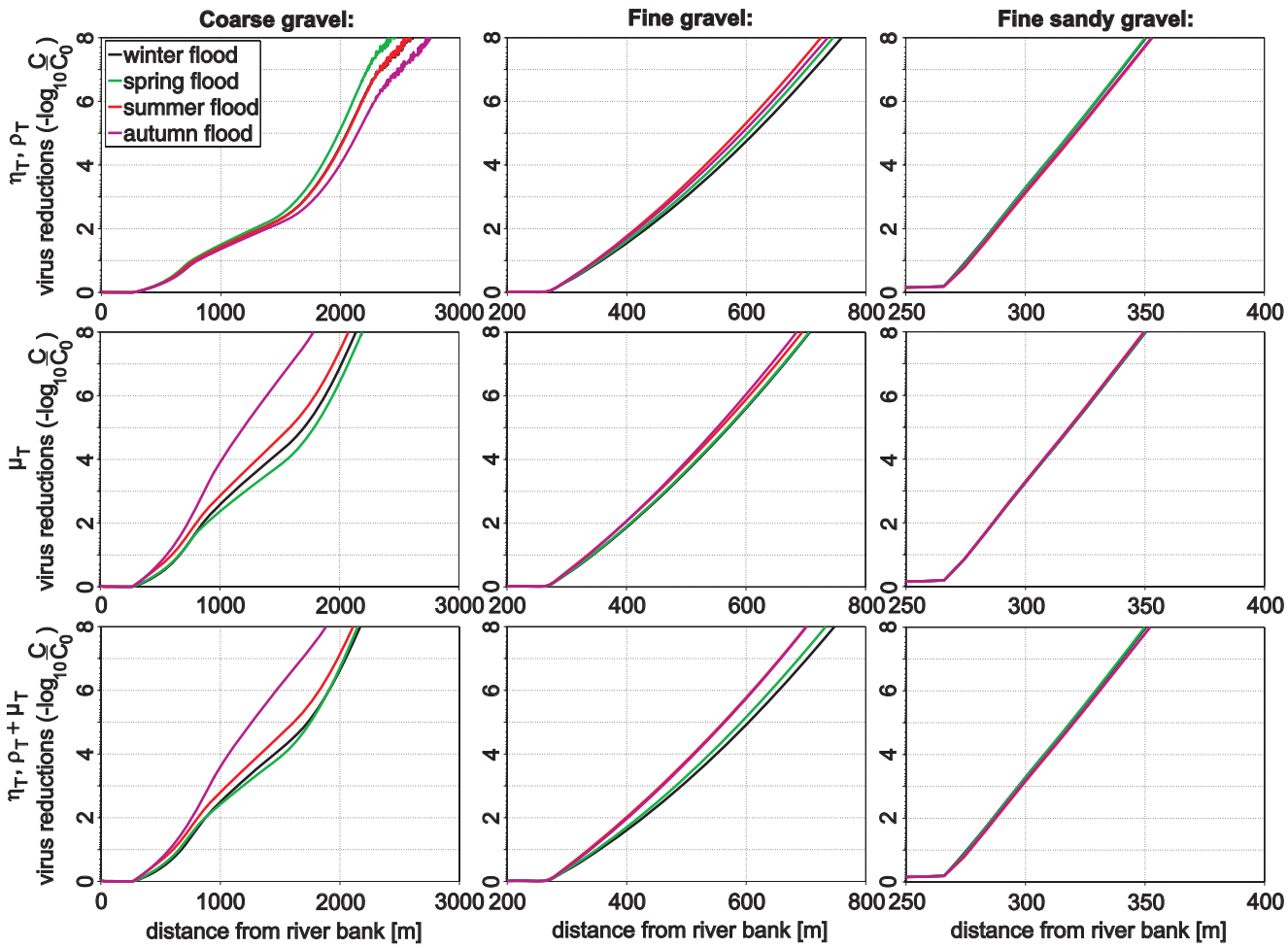

Fig. 6. Simulated minimum virus concentration reductions after 60 days of simulation time versus distance from the river bank (Fig. 9) for coarse gravel, fine gravel and fine sandy gravel material; For scenarios fluid viscosity (μ_T) and density (ρ_T) (top) and virus inactivation rate (η, middle) and all parameters together (bottom) were assigned dependent on water temperature. A pumping rate of 0 l/s is assumed. A virus concentration reduction at a respective distance from the river refers to an aquifer depth where the absolute minimum virus reduction at this point was simulated; Horizontal axis limits are set to where vertical axis limits are first reached.

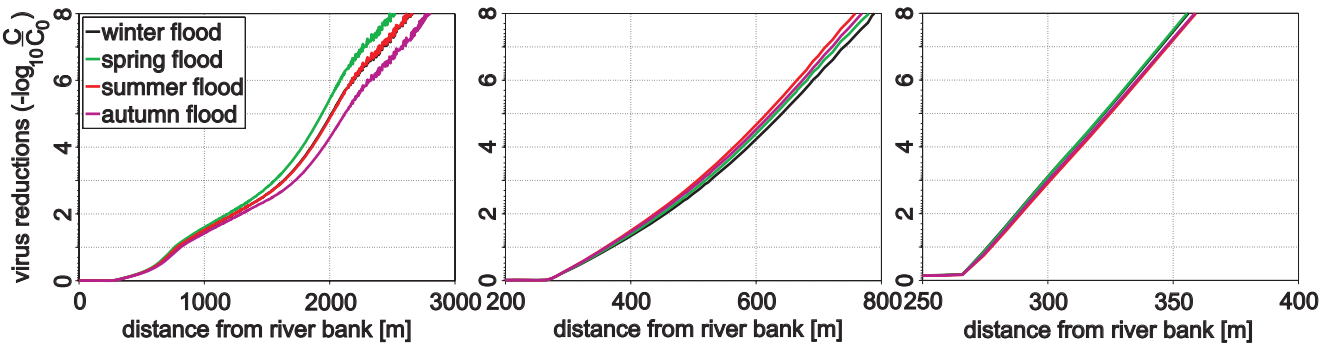

Fig. 7. Same as Figure 6 top, but with a pumping rate of 100 l/s;

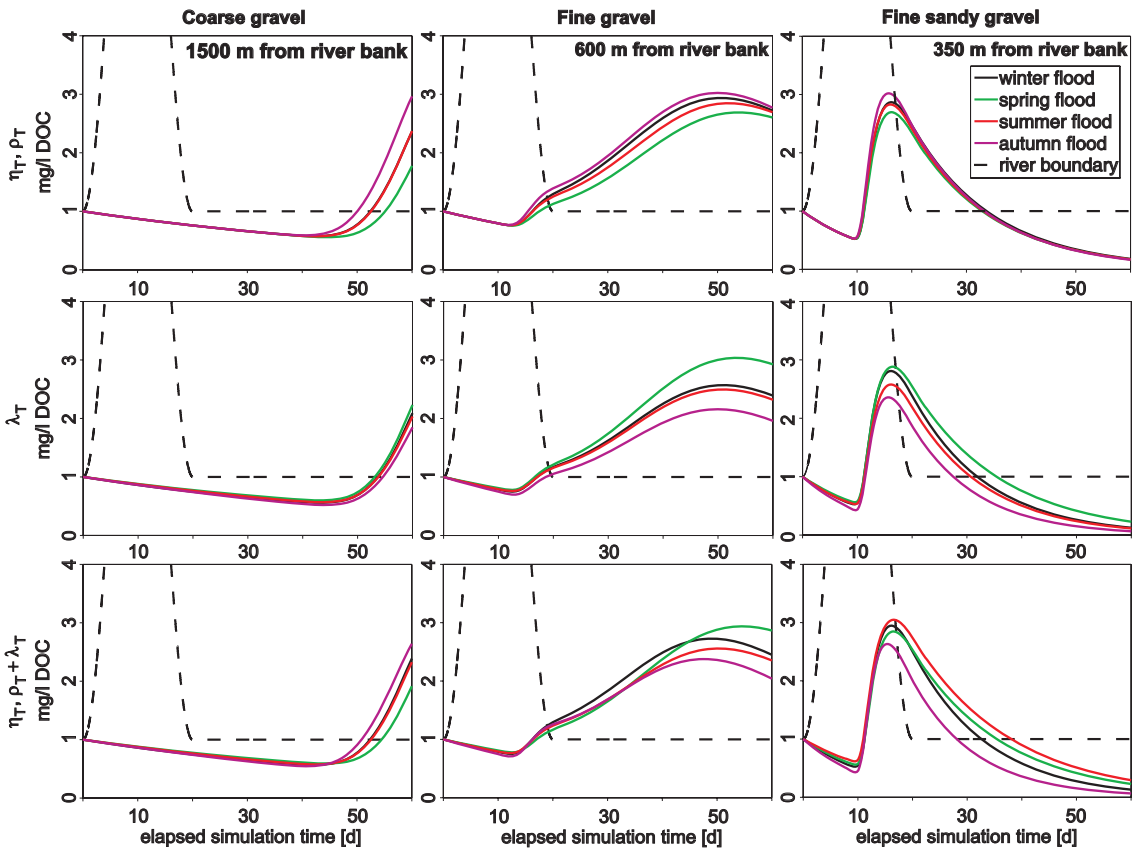

Fig. 8. Same as Figure 4, but for simulated DOC concentrations. Instead of virus inactivation rates, DOC decay rates (λ) were assumed dependent on water temperature (middle and bottom).

6. Discussion

6.1. Fluid viscosity and density effects combined with changing hydraulic conditions during floods

According to our simulation results, viscosity and density effects generally increase with the distance from the river (Fig. 6, top). Close to the river, virus and DOC concentrations are most likely more affected by variations in groundwater pressure gradients during the flood than by variations in water temperature. Derx et al. (2010) found that the magnitude of pore velocities in the near-river aquifer can vary strongly during flooding events. The lateral water level gradients varied from –0.3 to 0.3 % at their study site at the Danube, while a change in groundwater temperature from 2 °C to 22 °C at maximum could

Table 7. Minimum simulated virus concentration reductions and simulated peak DOC concentrations after 60 days for coarse gravel (Figs 6 and 9); For scenarios fluid viscosity (μ_T) and density (ρ_T) were assigned dependent on water temperature. Shown are the simulated values at the river boundary (0 m) and at various distances from the river bank (Fig. 1).

Coarse gravel Distances from river bank:	0 m	600 m	1100 m	1500 m	2500 m
virus $\log_{10} \frac{C}{C_0}$					
summer	0.0	0.5	1.6	2.3	7.6
autumn	0.0	0.5	1.5	2.2	6.9
winter	0.0	0.5	1.6	2.3	7.6
spring	0.0	0.6	1.7	2.4	8.2
peak DOC [%]					
summer	92.7	68.9	48.8	22.6	10
autumn	92.7	70.2	50.4	28.6	10
winter	91.8	69.6	49.0	22.6	10
spring	92.4	67.9	47.3	16.8	10

Table 8. Same as Table 7, but for fine gravel material.

Fine gravel Distances from river bank:	0 m	300 m	500 m	720 m
virus $\log_{10} \frac{C}{C_0}$				
summer	0.2	0.4	3.6	7.9
autumn	0.2	0.4	3.5	7.7
winter	0.2	0.4	3.2	7.2
spring	0.2	0.4	3.3	7.5
peak DOC [%]				
summer	84.9	96.1	37.9	18.4
autumn	84.9	96.3	39.8	20.5
winter	84.4	96.0	39.2	19.3
spring	85.0	95.7	36.4	16.3

cause a change in flow velocity due to viscosity changes by 57 % (Table 2).

Beside the effect on absolute concentration levels, changing fluid viscosities and densities over the seasons affected the simulated travel time of both types of contaminants. The simulated travel time was the shorter the warmer the groundwater temperature was assumed. Vogt et al. (2010) found a by up to 3 times shorter travel time from the river into groundwater at a restored compared to a channelised section of the River Thur. As the groundwater temperature was by approximately 2 °C higher at the restored section of the River Thur, viscosity and density effects may have been one responsible mechanism.

Table 9. Same as Table 7, but for fine sandy gravel.

Fine sandy gravel Distances from river bank:	0 m	100 m	300 m	350 m
virus $\log_{10} \frac{C}{C_0}$				
summer	0.9	0.2	3.2	9.6
autumn	0.9	0.2	3.2	9.6
winter	0.9	0.2	3.4	9.9
spring	0.9	0.2	3.4	10.0
peak DOC [%]				
summer	54.4	79.3	67.1	13.4
autumn	53.6	79.1	68.6	14.6
winter	55.1	76.4	66.9	13.6
spring	55.1	77.2	65.8	12.5

As the simulated transport distance in fine gravel was generally smaller than in coarse gravel, the simulated virus concentrations were most affected by groundwater temperature variations in the near-river aquifer during summer and winter (Fig. 6, centre). Simulated virus concentrations in fine gravel were more reduced after the summer flood which is likely due to turning groundwater flow directions during the receding flood, leading to temporary groundwater exfiltration into the river. Our results indicate that these conditions during a flood can lead to increased dilution processes because pristine groundwater is carried from further inland (arrows in Figs 1 and 5, centre).

Pumping can lead to more constant infiltration conditions from the river into groundwater, to higher groundwater gradients and thus to shorter travel times, as e.g. reported at the Great Miami River by Sheets et al. (2002). In accordance with these results, our simulations for fine gravel and fine sandy gravel material indicate that pumping can cause that virus concentrations are less effectively reduced during soil passage.

6.2. Effects of water temperature on virus removal, inactivation or DOC decay

In order to evaluate the net effects of seasonal changes in water temperature on contaminant removal, we considered changing fluid viscosities and densities and changes in virus inactivation rates. Our simulations demonstrate that virus concentrations can be reduced more effectively in warmer than in colder groundwater due to

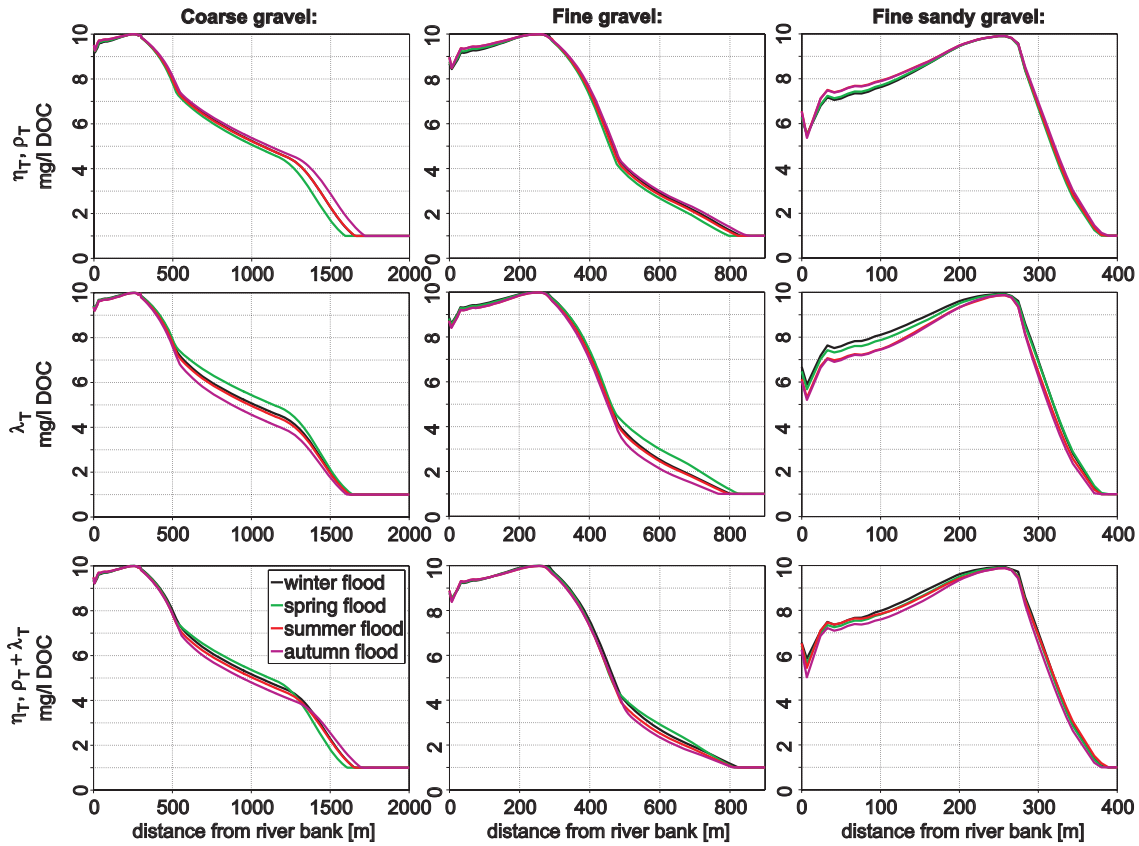

Fig. 9. Same as Figure 6, but for simulated DOC concentrations and an assumed DOC decay rate (λ) dependent on water temperature.

higher virus inactivation rates. Scenarios with a high assumed virus removal rate show that the effect of changing virus inactivation rates become negligible (Fig. 6, right).

In fact virus inactivation rates can vary strongly for different types of viruses also in relation to changes in water temperature. While the inactivation rate of e.g. *echo 1* strongly varies with water temperature (similarly as shown in our scenarios), *polio 1* or *HAV* do not show a significantly higher inactivation at warmer water temperatures (Schijven & Hassanizadeh 2000).

For such persistent types, our results indicate that fluid viscosity and density effects can cause that virus concentrations are reduced by up to 1.3 $\log_{10}\frac{C}{C_0}$ (16 %) less effectively during warmer seasons.

Virus removal rates may further increase with increasing water temperature according to colloid filtration theory (CFT, Yao et al. 1971). CFT predicts that virus particle movement during diffusion processes increases with increasing water temperature. As this theory, however, assumes a spherical shape of the collector particles and thus a uniform and well-sorted porous medium, it does not apply well for simulating virus transport in coarse gravel material. Moreover, gravel aquifers usually have a heterogeneous grain size distribution, and preferential flow processes may become more important than diffusion processes (Pang et al. 2005).

In contrast to virus inactivation, the effects of water temperature on simulated DOC concentrations appear to be clearer and less complex. Our simulations show that viscosity and density effects induced by changes in water temperature can counteract with effects of temperature dependent DOC decay rates in regards to DOC concentration levels. As a result DOC concentrations differ less between the seasons. The travel time, however, can be reduced by up to 14 % during warmer periods.

6.3. Implications for a more general case

Finally, the general implications of our simulation results for the consideration of contaminant removal during riverbank filtration are discussed. The groundwater temperature variations were clearly attenuated with distance, which is often observed in near-river groundwater

Table 10. Observed yearly range in water temperatures (°C) in various large rivers and adjacent groundwater (0–10 m below the river bed).

In river	≤ 200 m from river	≥ 200 m from river	Location	Reference
12–24	12–21		Russian, US	Su et al. (2004)
0–22	4–17	8–12	Elbe, Germany	Schoenheinz & Grischek (2011)
6–22	8–15		Rhine, Germany	Sontheimer (1991)
0–31	7–29		Great Miami, US	Sheets et al. (2002)
1–23	3–21	9–12	Danube, Austria	Fig. 2

(Schmidt et al. 2003, see Table 10). Advective flow, conduction and mixing are the responsible transport mechanisms (Sheets et al. 2002). The largest differences in simulated virus and DOC concentrations were between autumn and spring, as groundwater temperature was warmest in autumn and coldest in spring due to a time lag to the river water temperature. For deeper aquifers than assumed for our scenarios, the viscosity and density effects may be similar as shown in our simulations because the groundwater temperature fluctuations generally attenuate quickly with depth (Sheets et al. 2002, Su et al. 2004). While a simplified river geometry was assumed for our scenarios, river bed form heterogeneities, meanders and river side channels can further facilitate river-aquifer exchange (Storey et al. 2003, Cardenas 2008, Boano et al. 2010). In such cases groundwater temperature could respond stronger to changes in river water temperature. The changes in fluid viscosity and density induced by water temperature may consequently have stronger effects on virus and DOC transport. This may have important implications at restored river sections where the river bank geometry is in general more heterogeneous than assumed in our simulations (Vogt et al. 2010).

In cases of pronounced sediment clogging on top of the river bed and bank site, the viscosity and density effects on virus and DOC transport may diminish because groundwater temperature fluctuations become very small (Sheets et al. 2002). The same effects may be caused if groundwater is exfiltrating into the river during low flow conditions. During floods, however, river water infiltration often increases and sediment clogging may be partially removed, resembling the assumed conditions in our scenarios.

For our scenarios the river water was assumed to be saturated with oxygen. In the case of oxygen depletion, an increase in water temperature can further diminish the self-purification efficiency of the river bank sediments. With increasing microbial activity the oxygen consumption also increases. Oxygen depletion causes a transition from aerobic to anaerobic microbial degradation processes, which can cause the self-purification processes in the river bank to slow down significantly (Gross-Wittke et al. 2010).

7. Conclusion

We investigated the effects of changing fluid viscosities and densities, the effects of changing DOC decay rate and virus inactivation rates and their net effects on virus and DOC transport due to seasonal changes in groundwater temperature.

Our scenario results indicate that water temperature fluctuations can strongly affect virus and DOC removal during riverbank filtration. For DOC and a wide range of virus types the viscosity and density effects induced by water temperature changes can counteract with temperature dependent decay and inactivation rates.

Our simulations further indicate that fluid viscosity and density effects can result in a net decrease in virus removal efficiency for particular situations, such as for receding floods during colder periods. Moreover persistent types of viruses (e.g. *polio 1* or *HAV*) could be reduced less effectively (by up to 1.3 $\log_{10}\frac{C}{C_0}$) and may travel by up to 25 % faster during warmer than during colder periods.

We recommend considering viscosity and density effects induced by temperature changes in future studies investigating virus or DOC transport during riverbank filtration. The effects may be important specifically at field sites with a high river-aquifer exchange and large variations in groundwater temperature.

8. Acknowledgments

This paper was supported by the *Austrian Science Fund (FWF)* as part of the *DKplus* (*Vienna Doctoral Program on Water Resource Systems*, project number W1219) and the *GWRS-Vienna* in cooperation with Vienna Water as part of the *(New)Danube Untere Lobau Network Project* (*Gewässervernetzung (Neue) Donau Untere Lobau (Na-*

tionalpark Donau-Auen) funded by the Government of Austria (Federal Ministry of Agriculture, Forestry, Environment & Water Management), the Government of Vienna, and the European Agricultural Fund for Rural Development (project LE 07-13). We would like to thank the hydrology department of the Federal Waterway Authority, *viadonau – Österreichische Wasserstrassen-Gesellschaft mbH*, for providing the water temperature data in the Danube River. This publication was developed within the *Interuniversity Cooperation Centre Water and Health* (*ICC Water & Health*; www.waterandhealth.at).

9. References

Blaschke, A., Steiner, K.-H., Schmalfuss, R., Gutknecht, D. & Sengschmitt, D. (2003): Clogging processes in hyporheic interstices of an impounded river, the Danube at Vienna, Austria. – Int. Rev. Hydrobiol. **88**: 397–413.

Boano, F., Demaria, A., Revelli, R. & Ridolfi, L. (2010): Biogeochemical zonation due to intrameander hyporheic flow. – Water Resour. Res. **46**: 13 pp.

Boggs, J., Beard, L., Waldrop, W., Stauffer, T., MacIntyre, W. & Antworth, C. (1993): Transport of tritium and four organic compounds during a natural-gradient experiment (MADE-2). Technical Report EPRI-TR-101998 Palo Alto, CA.

Cardenas, M. (2008): The effect of river bend morphology on flow and timescales of surface water-groundwater exchange across pointbars. – J. Hydrol. **362**: 134–141.

Chen, X. (2000): Measurement of streambed hydraulic conductivity and its anisotropy. – Environ. Geol. **39**: 1317–1324.

de Marsily, G. (1986): Quantitative Hydrogeology. New York, Academic Press.

Derx, J., Blaschke, A.P. & Blöschl, G. (2010): Three-dimensional flow patterns at the river-aquifer interface – a case study at the Danube. – Advan. Water Res. **33**: 1375–1387.

Geiseler, G. (1967): D'Ans-Lax: Manual of practice for chemists and physicists (Taschenbuch für Chemiker und Physiker), vol. 1: Macroscopical physical-chemical properties. (Makroskopische physikalisch-chemische Eigenschaften). (3rd ed.) Berlin-Göttingen-New York, Springer Verlag.

Gelhar, L., Welty, C. & Rehfeldt, K. (1992): A critical review of data on field-scale dispersion in aquifers. – Water Resour. Res. **28**: 1955–1974.

van Genuchten, M. (1980): A closed-form equation for predicting the hydraulic conductivity of unsaturated soils. – Soil Sci. Soc. Am. J. **44**: 892–898.

Gross-Wittke, A., Gunkel, G. & Hoffmann, A. (2010): Temperature effects on bank filtration: redox conditions and physical-chemical parameters of pore water at Lake Tegel, Berlin, Germany. – J. Water and Climate Change **01**: 55–66.

Hoehn, E. (2002): Hydrogeological issues of riverbank filtration – a review. – In: Ray, C. (ed.), Riverbank filtration: understanding contaminant biogeochemistry and pathogen removal. – NATO Science Series, IV. Earth and Environmental Sciences **14**: 17–41.

Hoehn, E. & Scholtis, A. (2011): Exchange between a river and groundwater, assessed with hydrochemical data. – Hydrol. Earth Syst. Sci. 15: 983–988.

Homonnay, Z. (2002): Use of bank filtration in Hungary. – In: Ray, C. (ed.), Riverbank filtration: understanding contaminant biogeochemistry and pathogen removal. – NATO Science Series, IV. Earth and Environental Sciences **14**: 221–228.

Hubbs, S., Ball, K. & Caldwell, T. (2007): Technical Report 91141F AWWA Research Foundation.

Jekel, M., Grünheid, S., Baumgarten, B., Hübner, U. & Wiese, B. (2009): Removal of bulk and trace organics in underground treatment systems. – In: Micropol & Ecohazard 2009 – 6th IWA/GRA Specialized Conference on Assessment and Control of Micropollutants/Hazardous Substances in Water. San Francisco, CA: Groundwater Res. Assoc.

Kozeny, J. (1953): Hydraulics – basic principles and practical application. (Hydraulik. Ihre Grundlagen und praktische Anwendung). Vienna, Springer Verlag.

Kroiss, H., Matsché, N., Vogel, B., Zessner, M., Kavka, G., Farnleitner, A., Mach, R., Gutknecht, D., Blaschke, A., Heinecke, U., Hütter, T., Sengschmitt, D. & Steiner, K. (2002): Effects of infiltrating biologically treated wastewater on groundwater. (Auswirkungen der Versickerung von biologisch gereinigtem Abwasser auf das Grundwasser). Techn. Rep. Ministry for Economics and Labour, Ministry for Education, Science and Culture, Federal State Government Office of Burgenland, Sec. 9 – Water Surveillance, Ministry for Agriculture and Forestry, Environ. and Water Res. Manage. Vienna, Austria.

Krueger, C., Radakovich, K., Sawyer, T., Barber, L., Smith, R. & Field, J. (1998): Biodegradation of the surfactant linear alkylbenzenesulfonate in sewage-contaminated groundwater. A comparison of column experiments and field tracer tests. – Environ. Sci. Technol. **32**: 3954–3961.

Pang, L. (2009): Microbial removal rates in subsurface media estimated from published studies of field experiments and large intact soil cores. – J. Environ. Quality **38**: 1–12.

Pang, L., Close, M., Goltz, M., Noonan, M. & Sinton, L. (2005): Filtration and transport of *Bacillus subtilis* spores and the F-RNA phage MS2 in a coarse alluvial gravel aquifer: Implications in the estimation of setback distances. – J. Contam. Hydrol. **77**: 165–194.

Partinoudi, V. & Collins, M. (2007): Assessing RBF reduction/removal mechanisms for microbial and organic DBP precursors. – Journal AWWA **99**: 61–71.

Peyrard, D., Sauvage, S., Vervier, P., Sanchez-Perez, J. & Quintard, M. (2008): A coupled vertically integrated model to describe lateral exchanges between surface and subsurface in large alluvial floodplains with a fully penetrating river. – Hydrol. Process. **22**: 4257–4273.

Schijven, J.F. & Hassanizadeh, S. (2000): Removal of viruses by soil passage: Overview of modeling, processes and parameters. – Crit. Rev. Environ. Sci. Technol. **30**: 49–127.

Schmidt, C., Lange, F., Brauch, H.-J. & Kühn, W. (2003): Experiences with riverbank filtration and infiltration in Germany. Technical Report DVGW-Water Technology Center (TZW) Karlsruhe, Germany.

Schoenheinz, D. & Grischek, T. (2011): Behaviour of dissolved organic carbon during bank filtration under extreme climate conditions. – In: Ray, C. & Shamrukh, M. (eds.), Riverbank filtration for water security in desert countries. NATO Science for Peace and Security, C: Environmental Security (pp. 51–67). NATO Public Diplomacy Division.

Schubert, J. (2006): Significance of hydrologic aspects on RBF performance. – In: Hubbs, S. (ed.), Riverbank filtration hydrology number 60 in NATO Science (pp. 17–41).

Schwarzenbach, R., Giger, W., Hoehn, E. & Schneider, J. (1983): Behavior of organic compounds during infiltration of river water to groundwater. Field studies. – Environ. Sci. Technol. **17**: 472–479.

Shankar, V., Eckert, P., Ojha, C. & König, C. (2009): Transient three-dimensional modeling of riverbank filtration at Grind well field, Germany. – Hydrogeol. J. **17**: 321–326.

Sheets, R., Darner, R. & Whitteberry, B. (2002): Lag times of bank filtration at a well field, Cincinnati, Ohio, USA. – J. Hydrology **266**: 162–174.

Sim, Y. & Chrysikopoulos, C.V. (1998): Three-dimensional analytical models for virus transport in saturated porous media. – Transport in porous media **30**: 87–112.

Sontheimer, H. (1991): Drinking water from the Rhine? Report by a research project funded by the Federal Ministry for Research and Technology about the security of drinking water production from riverbank filtration at the Rhine River after impact loads (Trinkwasser aus dem Rhein? Bericht über ein vom Bundesminister für Forschung und Technologie gefördertes Verbundforschungsvorhaben zur Sicherheit der Trinkwassergewinnung aus Rheinuferfiltrat bei Stoßbelastungen). St. Augustin, Germany: Academia Verlag.

Stalder, G., Sommer, R., Walzer, C., Mach, R., Beiglböck, C., Blaschke, A. & Farnleitner, A. (2011): Hazard and risk based concepts for evaluating the microbial water quality – part 1 (Gefährdungs- und risikobasierende Konzepte zur Bewertung der mikrobiologischen Wasserqualität – Teil 1). – Wiener Tierärztliche Monatsschrift, Veterinary Medicine Austria **98**: 9–24.

Storey, R., Howard, K. & Williams, D. (2003): Factors controlling riffle-scale hyporheic exchange flows and their seasonal changes in a gaining stream: A three-dimensional groundwater flow model. – Water Resour. Res. **39***:* 1034.

Su, G., Jasperse, J., Seymour, D. & Constantz, J. (2004): Estimation of hydraulic conductivity in an alluvial system using temperatures. – Ground Water **42**: 890–901.

U.S. Army Corps of Engineers (2008): HEC-RAS – River analysis system. Technical Report Davis, CA.

via donau (1997): Die kennzeichnenden Wasserstände der österreichischen Donau (KWD 1996). Technical Report Vienna, Austria.

Vogt, T., Hoehn, E., Schneider, P., Freund, A., Schirmer, M. & Cirpka, O. (2010): Fluctuations of electric conductivity as a natural tracer for bank filtration. – Adv. Water Resour. **33**: 1296–1308.

Voss, C.I. & Provost, A.M. (2008): SUTRA – a model for saturated – unsaturated variable density ground water flow with solute or energy transport. Technical Report Water-Resources Investigations Report 02-4231 Reston, Virginia.

Weiss, W., Bouwer, E., Aboytes, R., LeChevallier, M., O'Melia, C., Le, B. & Schwab, K. (2005): Riverbank filtration for control of microorganisms: Results from field monitoring. – Water Res. **39**: 1990–2001.

Weiss, W., Bouwer, E., Ball, W., O'Melia, C., LeChevallier, M., Arora, H. & Speth, T. (2003): Riverbank filtration-Fates of DBP precursors and selected microorganisms. – J. Am. Water Works Assoc. **95**: 68–81.

Wolfram, G. & Humpesch, U. (eds.) (2003): New Danube 2002: Effects of differently high water events on the New Danube. City of Vienna *MA45* and the Austrian Hydro Power AG (*Verbund*).

Wolfram, G. & Humpesch, U. (eds.) (2004): New Danube 2003 – a well balanced ecosystem. City of Vienna *MA45* and the Austrian Hydro Power AG (*Verbund*).

Wolfram, G. & Humpesch, U. (eds.) (2005). New Danube 2004. 2 years without high water inflows – Best water quality since 1987. City of Vienna *MA45* and the Austrian Hydro Power AG (*Verbund*).

Yao, K., Habibian, M. & O'Melia, C. (1971): Water and waste water filtration: concepts and applications. – Environ. Sci. Technol. **5**: 1105–1112.

Received 23 December 2011
Modified version received 2 April 2012
Accepted 4 July 2012